Inorganic Chemistry

Communication

pubs.acs.org/IC

Comparative Study of Activation Methods on Tuning Gas Sorption Properties of a Metal–Organic Framework with Nanosized Ligands

Yan-Ping He, Yan-Xi Tan, and Jian Zhang*

State Key Laboratory of Structural Chemistry, Fujian Institute of Research on the Structure of Matter, Chinese Academy of Sciences, Fuzhou, Fujian 350002, P. R. China

Supporting Information

ABSTRACT: Presented here is a new porous metal–organic framework based on a nanosized tris((4-carboxyl)-phenylduryl)amine ligand, which features a 2-fold interpenetrating **hms** network and shows distinct gas adsorption behaviors dependent on different activation methods.

Recently, porous metal–organic framework materials (MOFs) have been considered as very promising candidate for gas storage and separation because of their permanent microporosity and large internal surface areas.[1] For general applicability, MOFs should have high thermal stability to keep permanent porosity after removal of the solvent molecules.[2] Unfortunately, frameworks constructed from the large ligands often collapse or distort into nonporous frameworks upon guest removal by conventional activation methods such as evacuation or heating. Therefore, how to retain the pores and avoid structural shrinking may be extremely challenging. Up to now, some activated treatment methods, such as heat activation,[3] solvent-exchange,[4] and supercritical carbon dioxide (SCD),[5] have been recognized as effective physical approaches to enhance the permanent porosity of MOFs. For example, Suh's group successfully tuned the N_2 uptakes of IRMOF-3 by conventional heating activation, $CHCl_3$ exchange, and SCD activation.[1a] Recently, Lin and his co-workers reported another special freeze-benzene drying treatment method to improve the surface areas of two MOFs.[6] Compared to the use of toxic benzene, cyclohexane may be a more suitable choice for such freeze-drying treatment. Moreover, cyclohexane has very weak interaction with many aromatic host frameworks, so that the guest removal process must be easy too. However, little experimental effort has been concerned with the use of a freeze-cyclohexane drying treatment to tune porosity of MOFs for gas sorption.

In this work, we first employ such a freeze-cyclohexane drying treatment to activate the porosity of a new porous MOF, namely $[Zn_2L(Im)]\cdot 7(DMF)$ (**FIR-3**; L = Tris((4-carboxyl)-phenylduryl)amine, Im = imidazole, DMF = N,N-dimethylformamide; **FIR** denotes Fujian Institute of Research). As a novel nanosized ligand, tris((4-carboxyl)phenylduryl)amine is rarely explored to construct MOFs with satisfying stability.[7] Compound **FIR-3** reported here features a 2-fold interpenetrating pillared layer structure where the short Im ligands act as the pillars. Three different activation methods, such as solvent-exchange, freeze-cyclohexane drying, and SCD activation, were carefully performed to investigate their impact on the tuning porosity of **FIR-3**.

Crystals of **FIR-3** were prepared using the solvothermal reaction of $Zn(NO_3)_2\cdot 6H_2O$, Im, and H_3L in DMF/ethanol (3:1, v/v).[8] Single-crystal X-ray diffraction reveals that **FIR-3** crystallized in the space group $C2/c$.[9] The L ligand looks like a propeller because the average dihedral angle between two duryl planes is 21.5°, and that between the duryl plane and the outer phenyl plane is 63.1° (Figure 1). The central N atom of L exhibits sp^2 hybridization, showing C–N–C average angles of 120.0° and short N–C bond lengths (average 1.417 Å). In the structure of **FIR-3**, each Zn center is four-coordinate with three carboxylate O atoms from three different L ligands and one N atom from an Im ligand, showing tetrahedral geometry. Two tetrahedral Zn centers are bridged by three carboxylate groups to form a $Zn_2(COO)_3$ unit with Zn···Zn distance of 3.3789(5) Å. This $Zn_2(COO)_3$ unit is interesting and rarely observed in other coordination compounds.[10] Each L ligand links to three $Zn_2(COO)_3$ units in a bidentate fashion, forming a layer with a hexahydric ring giving a border length of about 12.4 Å (Figure 2a). Each layer can be topologically represented as a uninodal

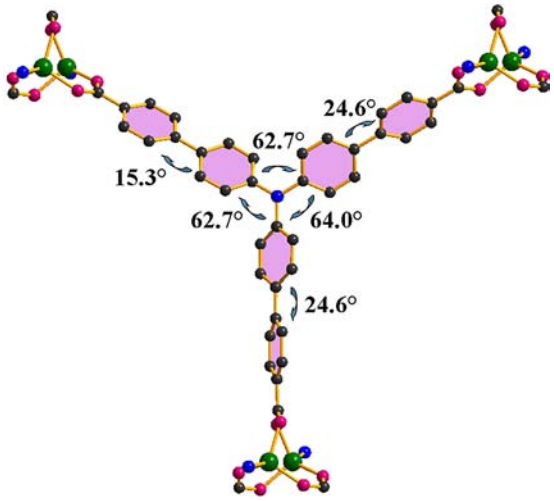

Figure 1. Coordination environment in **FIR-3** (Zn, green; C, black; O, red; N, blue).

Received: August 9, 2012
Published: October 8, 2012

   dx.doi.org/10.1021/ic3017529 | *Inorg. Chem.* 2012, 51, 11232–11234

three-connected **hcb** net by reducing each L ligand and each $Zn_2(COO)_3$ unit into three-connected nodes (Figure 2a).

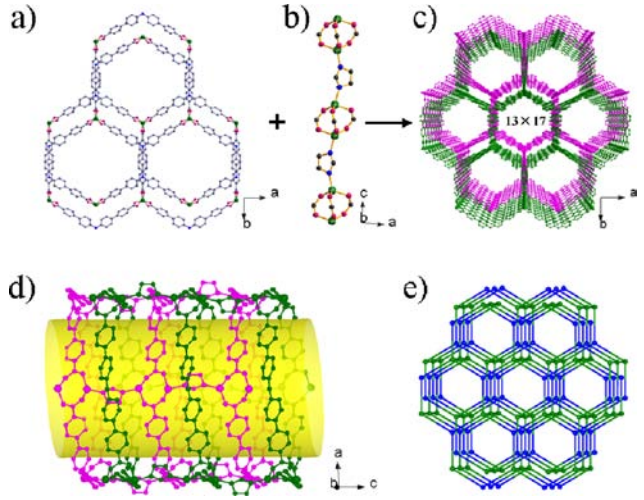

Figure 2. (a) The **hcb**-type layer in **FIR-3**. (b) The chain with $Zn_2(COO)_3$ units linked by the Im ligands. (c) The 2-fold interpenetrating framework of **FIR-3**. (d) The channel in **FIR-3**. (e) The 2-fold interpenetrating (3,5)-connected **hms** net derived from the structure of **FIR-3**.

Interestingly, the $Zn_2(COO)_3$ units are further connected by the Im ligands into infinite chains along the *c* axis (Figure 2b). Through the Im ligand, the **hcb**-type layers are further pillared into a 3D framework with the biggest pore size of 18.5 Å along the *c* axis (Figure 2d). The large intraframework spaces are occupied by another identical but independent framework, giving a 2-fold interpenetrating structure (Figure 2c). Considering the bridging Im ligands, each $Zn_2(COO)_3$ unit acts as a five-connected node, and the trigonal L ligand keeps its three-connectivity. Thus, the network topology of **FIR-3** can be described as a (3,5)-connected **hms** net (Figure 2e).

Despite the 2-fold interpenetration, the whole structure still shows honeycomb-like channels with an effective window size of 13 × 17 $Å^2$ along the *c* axis (Figure 2d). The solvent-accessible volume of **FIR-3** is estimated by the PLATON program to be about 62.0% of the total crystal volume. The free spaces are occupied by the structurally disordered solvent molecules. Thermogravimetric analysis (TGA) on the as-synthesized sample of **FIR-3** indicated a weight loss of 39.47% in the temperature range 20−350 °C (Figure S3, Supporting Information), which is consistent with the release of seven DMF guest molecules per $Zn_2L(Im)$ unit.

For gas adsorption studies, the sample of **FIR-3** was completely exchanged by dichloromethane (CH_2Cl_2) after soaking **FIR-3** in CH_2Cl_2 under ambient conditions for 48 h, and the CH_2Cl_2-exchanged sample was further activated by heating at 30 °C for 12 h under vacuum conditions, giving a hollow framework **FIR-3a-ht**. The powder X-ray diffraction (PXRD) pattern of **FIR-3a-ht** is obviously changed, as compared to that of the as-synthesized sample, which indicates that framework distortion or structural transformation may occur (Figure S4, Supporting Information). It can be attributed to the detrimental effect of surface tension in inducing nanopore collapse during the vacuum process.

In order to avoid the MOF framework experiencing the deleterious effect of solvent surface tension, a freeze-drying experiment was carried out. The sample of **FIR-3** was dipped in cyclohexane (C_6H_{12}) at 60 °C, and this process was repeated every 24 h for 3 days, forming a fully C_6H_{12}-loading sample **FIR-3b** attested by TGA. The suspension of **FIR-3b** in C_6H_{12} was transferred to a sample cell. After being frozen at 0 °C about 5 h, the sample cell was placed under dynamic vacuum conditions in an ice/H_2O bath for 24 h, and the included solvent molecules underwent sublimation in the freeze-drying process. A hollow phase of **FIR-3b-ht** was obtained, and the TGA measurement confirmed that all of the C_6H_{12} had been removed during the freeze-drying course. The PXRD pattern of **FIR-3b-ht** was much better than that of **FIR-3a-ht**, but the PXRD pattern becomes broad and a shift in peak positions happens.

To attain a more complete evacuation and best structural integrity, SCD was used to activate the original **FIR-3a**, and the third new hollow phase **FIR-3c-ht** was obtained. Compared to the as-synthesized sample, structural change was also observed, but that is much better than those of **FIR-3a-ht** and **FIR-3b-ht**. These results illustrate that framework distortion or shrinking is always present in this interpenetrating framework.

Different activation treatments of **FIR-3** provide a great opportunity to make a comparative study on tuning porosity for gas sorption. First, the N_2 adsorption isotherms for activated samples of **FIR-3a-ht**, **FIR-3b-ht**, and **FIR-3c-ht** were collected to determine how the activation treatment impacts the pore volume and surface area (Figure 3). The N_2 sorption isotherm

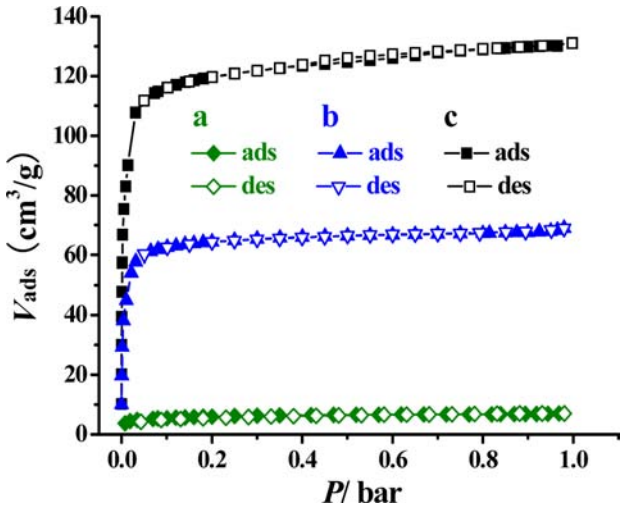

Figure 3. N_2 sorption isotherms for **FIR-3a-ht** (a), **FIR-3b-ht** (b), and **FIR-3c-ht** (c) at 77 K.

shows that the desolvated solid **FIR-3a-ht** can hardly adsorb N_2 at 77 K. However, the isotherms of **FIR-3b-ht** and **FIR-3c-ht** reveal reversible type-I adsorption/desorption behaviors, demonstrating their permanent microporosity. The BET and Langmuir surface areas as well as the micropore volumes of **FIR-3a-ht**, **FIR-3b-ht**, and **FIR-3c-ht** are listed in Table 1. The results are all consistent with the anticipation. The more that mild active conditions were used, the greater the pore volume and surface area of an active framework that could be obtained. The Langmuir surface area increased to 288.6 m^2/g for the freeze-dried sample of **FIR-3b-ht** and 544.3 m^2/g for the supercritical CO_2 dried sample of **FIR-3c-ht**, which are about an 11 times and 20 times enhancement over the regular vacuum-dried sample **FIR-3a-ht**. However, they are all greatly

dx.doi.org/10.1021/ic3017529 | *Inorg. Chem.* 2012, 51, 11232−11234

Table 1. Sorption Data for FIR-3 under Different Activation Methods

compounds	langmuir[a]	BET[a]	Vp[b]
FIR-3a-ht	29.4	24.3	0.01
FIR-3b-ht	288.6	266.0	0.11
FIR-3c-ht	544.3	497.2	0.20

[a]Surface area, m^2/g, [b]Vp is the measured pore volume, cm^3/g.

lower than the theoretical surface area of 1722.6 m^2/g calculated by Materials Studio 5.0. Single point adsorption total pore volumes at P = 0.98 bar from the N_2 sorption are 0.01 cm^3/g for **FIR-3a-ht**, 0.11 cm^3/g for **FIR-3b-ht**, and 0.20 cm^3/g for **FIR-3c-ht**, which are all much lower than that of 0.902 cm^3/g estimated from the single crystal structure. The lower surface area and pore volumes indicate that the host framework appears to undergo significant pore collapse regardless of the activation method. However, the degree of pore collapse appears to be less when activated with supercritical CO_2 or the cyclohexane freeze/pump method. The surface areas are only a small fraction of what is predicted based on their structures. The above results indicate that the elimination of the detrimental effect of surface tension can avoid the collapse or shrinking of porous framework, thereby enhancing the permanent porosity and gas uptake of MOFs.[5,6,11]

The CO_2 sorption isotherms were also measured at 273 K (Figure 4). The CO_2 uptakes of these compounds follow a similar increasing trend. As shown in Figure 4, the adsorption and desorption isotherm curves do not overlap with each other with small hysteresis. The capacity of **FIR-3c-ht** to adsorb CO_2 is 33.1 cm^3/g at 273 K and 1 bar, a value surpassing that of **FIR-3b-ht** (23.8 cm^3/g) and **FIR-3a-ht** (17.0 cm^3/g).

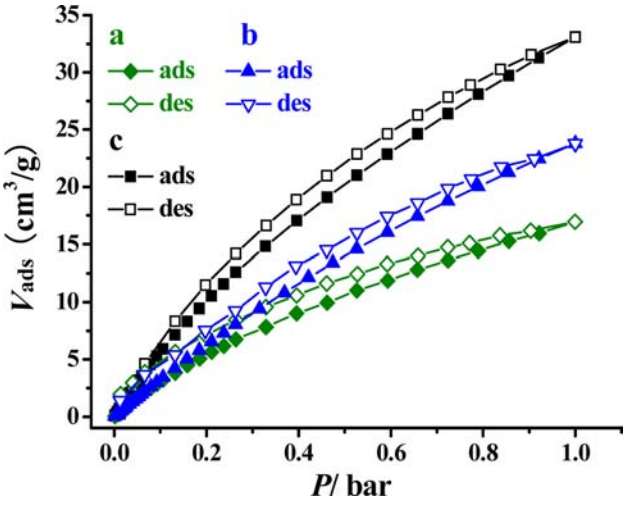

Figure 4. CO_2 sorption isotherms for **FIR-3a-ht** (a), **FIR-3b-ht** (b), and **FIR-3c-ht** (c) at 273 K.

In summary, a comparative study of activation methods on tuning gas sorption properties of **FIR-3** with a nanosized tris[(4-carboxyl)phenylduryl]amine ligand is successfully investigated. A novel freeze-cyclohexane drying treatment was used to improve the porosity of MOFs for the first time. The results demonstrate the importance of activation treatment on controlling the framework stability and porosity.

■ ASSOCIATED CONTENT

Supporting Information

Experimental details, additional figures, TGA, powder X-ray diffraction patterns, IR spectra, and a CIF file. This material is available free of charge via the Internet at http://pubs.acs.org.

■ AUTHOR INFORMATION

Corresponding Author

*E-mail: zhj@fjirsm.ac.cn.

Notes

The authors declare no competing financial interest.

■ ACKNOWLEDGMENTS

This work is supported by the 973 program (2011CB932504 and 2012CB821705), NSFC (21073191, 21221001), NSF of Fujian Province (2011J06005), and CAS.

■ REFERENCES

(1) (a) Suh, M. P.; Park, H. J.; Prasad, T. K.; Lim, D. W. *Chem. Rev.* **2012**, *112*, 782. (b) Liu, J.; Thallapally, P. K.; McGrail, B. P.; Brown, D. R.; Liu, J. *Chem. Soc. Rev.* **2012**, *41*, 2308. (c) Yang, S.; Lin, X.; Blake, A. J.; Walker, G.; Hubberstey, P.; Champness, N. R.; Schröder, M. *Nat. Chem.* **2009**, *1*, 487. (d) Lin, Q.; Wu, T.; Zheng, S.; Bu, X.; Feng, P. *Chem. Commun.* **2011**, *47*, 11852. (e) Jiang, H. L.; Xu, Q. *Chem. Commun.* **2011**, *47*, 3351. (f) Chen, B. L.; Xiang, S. C.; Qian, G. D. *Acc. Chem. Res.* **2010**, *43*, 1115−1124.

(2) (a) AlmeidaPaz, F. A.; Klinowski, J.; Vilela, S. M.; Tomé, J. P.; Cavaleiroc, J. A.; Rocha, J. *Chem. Soc. Rev.* **2012**, *41*, 1088. (b) Xue, Y. S.; He, Y. B; Ren, S. B.; Yue, Y. F.; Zhou, L.; Li, Y. Z.; Du, H. B.; You, X. Z.; Chen, B.-L. *J. Mater. Chem.* **2012**, *22*, 10195. (c) Zheng, S.; Wu, T.; Zuo, F.; Chou, C T.; Feng, P.; Bu, X. *J. Am. Chem. Soc.* **2012**, *134*, 1934. (d) Jiang, H. L.; Tatsu, Y.; Lu, Z. H.; Xu, Q. *J. Am. Chem. Soc.* **2010**, *132*, 5586.

(3) (a) Tan, Y. X.; Wang, F.; Kang, Y.; Zhang, J. *Chem. Commun.* **2011**, *47*, 770. (b) Zheng, S. T.; Bu, J. T.; Li, Y. F.; Wu, T.; Zuo, F.; Feng, P. Y.; Bu, X. H. *J. Am. Chem. Soc.* **2010**, *132*, 17062.

(4) (a) Tan, Y.-X.; He, Y.-P.; Zhang, J. *Inorg. Chem.* **2011**, *50*, 11527. (b) Mu, B.; Li, F.; Huang, Y. G.; Walton, K. S. *J. Mater. Chem.* **2012**, *22*, 10172. (c) Zheng, B.-S.; Bai, J. F.; Duan, J.-G.; Wojtas, L.; Zaworotko, M. J. *J. Am. Chem. Soc.* **2011**, *133*, 748.

(5) (a) Nelson, A. P.; Farha, O. K.; Mulfort, K. L.; Hupp, J. T. *J. Am. Chem. Soc.* **2009**, *131*, 458. (b) Farha, O. K.; Hupp, J. T. *Acc. Chem. Res.* **2010**, *43*, 1166. (c) Cooper, A. I.; Rosseinsky, M. J. *Nat. Chem.* **2009**, *1*, 26. (d) Han, D.; Jiang, F. L.; Wu, M. Y.; Chen, L.; Chen, Q. H.; Hong, M.-C. *Chem. Commun.* **2011**, *47*, 9861.

(6) Ma, L.-Q.; Jin, A.; Xie, Z. G.; Lin, W. B. *Angew. Chem., Int. Ed.* **2009**, *48*, 9905.

(7) (a) He, Y. P.; Tan, Y. X.; Wang, F.; Zhang, J. *Inorg. Chem.* **2012**, *51*, 1995. (b) Tan, Y. X.; He, Y. P.; Zhang, J. *Cryst. Growth Des.* **2012**, *12*, 2468. (c) Park, H. J.; Lim, D. W.; Yang, W. S.; Oh, T. R.; Suh, M. P. *Chem.—Eur. J.* **2011**, *17*, 7251.

(8) See Supporting Information.

(9) See Supporting Information.

(10) (a) Wu, M. Y.; Jiang, F. L.; Wei, W.; Gao, Q.; Huang, Y. G.; Chen, L.; Hong, M. C. *Cryst. Growth Des.* **2009**, *9*, 2559. (b) Rood, J. A.; Boggess, W. C.; Noll, B. C.; Henderson, K. W. *J. Am. Chem. Soc.* **2007**, *129*, 13675. (c) Wang, X. S.; Chrzanowski, M.; Gao, W. Y.; Wojtas, L.; Chen, Y. S.; Zaworotko, M. J.; Ma, S. Q. *Chem. Sci.* **2012**, *3*, 2823.

(11) (a) Farha, O. K.; Yazaydin, A. O.; Eryazici, I.; Malliakas, C. D.; Hauser, B. G .; Kanatzidis, M. G.; Nguyen, S. T.; Snurr, R. Q.; Hupp, J. T. *Nat. Chem.* **2010**, *2*, 944. (b) Lohe, M. R.; Rose, M.; Kaskel, S. *Chem. Commun.* **2009**, *45*, 6056. (c) Doonan, C. J.; Morris, W.; Furukawa, H.; Yaghi, O. M. *J. Am. Chem. Soc.* **2009**, *131*, 9492.